ELSEVIER

Biophysical Chemistry 59 (1996) 107–117

Biophysical Chemistry

Oxygen binding to fallow-deer (*Dama dama*) hemoglobin: stepwise enthalpies at pH 7.4

Craig R. Johnson [a,*], Mauro Angeletti [b], Stefania Pucciarelli [b], Ernesto Freire [a]

[a] *Department of Biology and Biocalorimetry Center, The Johns Hopkins University, Baltimore, MD 21218, USA*
[b] *Department of MCA Biology, University of Camerino, Camerino, Italy*

Received 18 April 1995; revised 7 November 1995; accepted 14 November 1995

Abstract

High-precision thin-layer gas-solution microcalorimetry has been used to study the oxygen binding properties of fallow-deer (*Dama dama*) hemoglobin under physiological conditions. This method measures directly the enthalpy of macromolecular ligand binding by changing the ligand activity in a manner analogous to that of the Gill thin-layer optical apparatus ([1], D. Dolman and S.J. Gill, Anal. Biochem., 87 (1978) 127–134). By logarithmically lowering the partial pressure of oxygen we have generated differential heat binding curves of oxygen binding to fallow-deer hemoglobin in phosphate buffer at pH 7.4. In order to enlarge the data field, the temperature dependence of the oxygen affinity was examined by generating binding curves at a number of different temperatures allowing for separation of enthalpy and free energy parameters. This type of experimental analysis makes no assumption of optical linearity between the various heme groups and reveals initially that overall oxygen binding to fallow-deer hemoglobin is less exothermic and of lower affinity than for human hemoglobin A_0. In addition, previous optical work on the ancestrally related reindeer hemoglobin (*Rangifer tarandus*; [2], B. Giardina, O. Brix, M. Nuutinen, S. Sherbini, A. Bardgard, G. Lazzarino and S. Condo, FEBS Lett., 247 (1989) 135) has indicated that the enthalpy associated with its final two oxygen binding steps is minimal. Our calorimetric determination with fallow-deer hemoglobin also reveals this tendency. Presumably, this adaptation would make it easier for these animals to maintain a consistent hemoglobin oxygen saturation level under environmental conditions where the temperature fluctuates.

Keywords: Calorimetry; Allosteric interactions; Cooperativity; Molecular adaptation; Hemoglobin; Oxygen binding

1. Introduction

For many years tetrameric hemoglobins from a large number of species have been studied as model systems that demonstrate many of the structural and functional characteristics present in all proteins [3,4]. In addition to being readily available in large quantities hemoglobins have a number of attractive properties which make them ideally suited for experimental analysis. These characteristics include high stability and solubility, intense optical spectra, excellent crystal forming properties, and a number of well documented functional characteristics. The fundamental ideas concerning allosteric [5–8], polysteric [9] and polyphasic [10] molecular regulation were initially

* Corresponding author.

SSDI 0301-4622(95)00140-9

probed through the study of the ligand binding processes associated with different species and mutants of hemoglobin. A general description of the basic properties of heme proteins can be found in a number of classical reviews [11–13]. In addition, there are a number of more specific reviews pertaining to hemoglobins structural [14–17] and functional properties [18,19].

The functional characteristics of respiratory proteins are best represented by examining the changes in gaseous binding curves in the presence of allosteric effectors such as protons, organic phosphates, carbon dioxide and chloride. In general, the interpretation of binding curves allows for the determination of the fundamental thermodynamic properties associated with particular macromolecular ligand binding systems [20,21]. When these types of thermodynamic characteristics are combined with structural information, models can be formulated that relate the various structural features of hemoglobins to their functional properties. Recently, mutant and partially ligated hemoglobins were used to reveal cooperativity between the α and β subunit hemes in each dimeric half of human hemoglobin [18,22]. This analysis led to the discovery of a symmetry rule in which quaternary T to R state switching appears to occur when heme site binding yields at least one ligated subunit on each side of the dimer–dimer interface. In this paper we examine the functional characteristics of fallow-deer hemoglobin in an attempt to explore how physiological constraints may dictate the selection of particular structures.

The experiments presented here are designed to eliminate the uncertainty attributed to possible nonlinear optical effects believed to exist in spectral determinations [23]. A high-precision thin-layer gas-solution microcalorimeter is used which utilizes millimolar concentrations of heme in microliter quantities while exhibiting microjoule sensitivity [24,25]. This method is a purely enthalpic approach and does not require any assumption of optical linearity between the various heme groups. Previously, this instrument was used to determine the complete stepwise thermodynamics associated with oxygen binding to human as well as bovine hemoglobin under physiological conditions [26]. The same type of analysis will be applied in this paper to fallow-deer hemoglobin.

2. Materials and methods

2.1. General preparations

Fallow-deer hemoglobin samples were prepared using a modification of the purification scheme of Riggs [27] described for human hemoglobin. Briefly, after cell lysis and removal of stroma the lysate was dialyzed against 20 mM Tris(hydroxymethyl)aminomethane hydrochloride (Tris–HCl) and then applied to a diethylaminoethyl (DEAE)–Sephadex A-50 column (4×60 cm), previously equilibrated with the same buffer. Elution was conducted using a NaCl gradient in 20 mM Tris–HCl at pH 9.1. The resulting hemoglobin, less than 3% met-hemoglobin (methoxy hemoglobin, oxidized hemoglobin) was dialyzed at 4°C for 24 h in 0.2 M potassium phosphate and 1 mM ethylenediaminetetraacetic acid (EDTA) at pH 7.4. Phosphate buffer was chosen for its small protonation heat of approximately -0.8 kcal/mol [28]; this is important as most hemoglobins exhibit large Bohr effects upon oxygen binding. Purified protein samples were stored as pellets in liquid nitrogen until ready for use. The enzyme reducing system of Hayashi [29] was used to reduce met-hemoglobin formation (Table 1), and its components were purchased from Sigma and placed in the appropriate buffer before addition to the heme solutions. The samples were checked for alteration in pH before beginning the experiment.

Hemoglobin concentrations were determined using a previously calibrated thin-layer optical cell (0.0101 cm) placed in a Perkin-Elmer Lambda 4B spectrophotometer. To obtain accurate reduced hemoglobin concentrations, absorbance readings were taken at a number of different wavelengths and the following analysis was applied. For a mixture of components [as in the case of methoxy, oxy (reduced

Table 1
Extinction coefficients for species of fallow-deer hemoglobin in 0.2 M potassium phosphate, 1 mM EDTA at pH 7.4

	λ (nm)				
	540	560	570	576	630
ε (oxy)	13.82	8.0	11.64	15.06	0.15
ε (dcoxy)	8.46	10.09	8.63	7.4	0.46
ε (met)	6.84	3.97	4.67	5.3	1.98

hemoglobin with oxygen bound) and deoxy (reduced hemoglobin with no oxygen bound) forms of hemoglobin], the absorbance value at a given wavelength can be represented by a generalized Lambert–Beer law, the total absorbance being a linear combination of the contributions of the n components. For each component concentration C_i and extinction coefficient $\varepsilon_{\lambda,i}$ the absorbance contribution for that species at a particular wavelength λ is given as

$$A_\lambda = b \sum_{i=1}^{n} \varepsilon_{\lambda,i} C_i \qquad (1)$$

where b is the path length of the spectrophotometric cell. If we determine the extinction coefficients for each particular species i at a number of different wavelengths, the composition of a mixture of these species can be determined by recording the absorbance readings of the mixture at these wavelengths. As with human hemoglobin [30,31], fallow-deer extinction coefficients were determined at 540, 560, 570, 576 and 630 nm. These wavelengths correspond to the characteristic peaks for oxyhemoglobin (540, 576), deoxyhemoglobin (560), carboxyhemoglobin (540, 570) and met-hemoglobin (540, 576, 630).

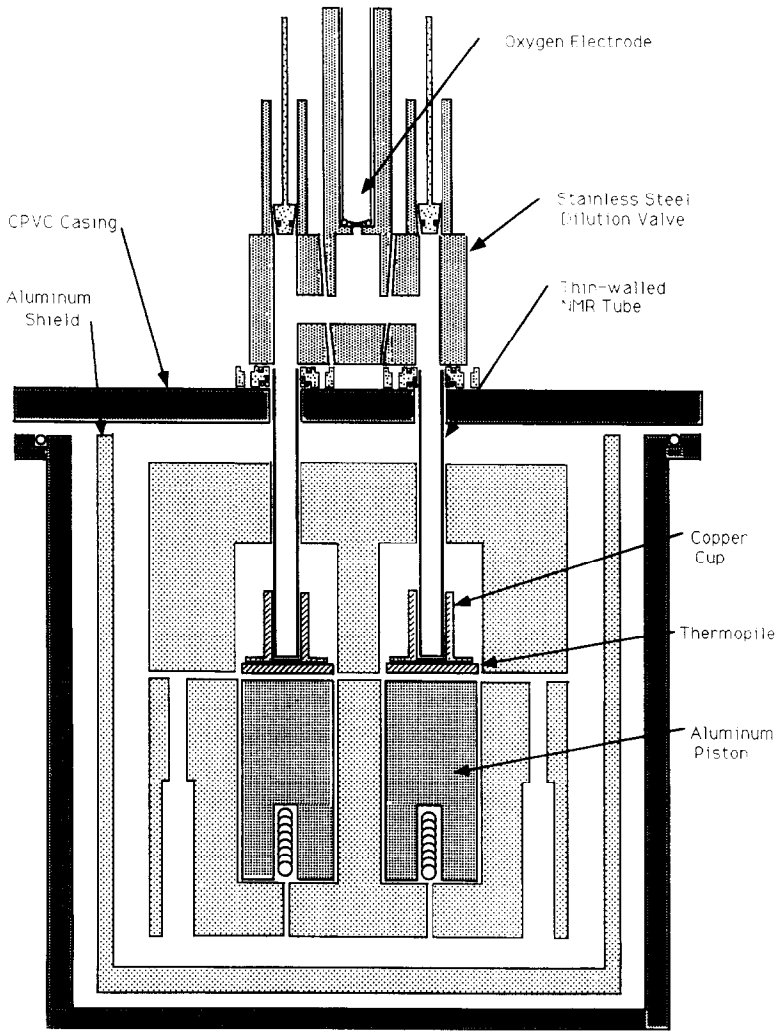

Fig. 1. Calorimeter and gas dilution valve.

In order to determine the extinction coefficients of a particular species, the absorbance readings of the pure component are taken at the appropriate wavelengths, followed by total heme content analysis via the pyridine–hemochromogen complex method [32]. In this procedure all forms of heme are converted to the complex by first adding pyridine to the hemoglobin solution followed by the addition of $Na_2S_2O_4$. When the pyridine–hemochromogen complex forms, absorbances at 557 nm ($\varepsilon_{557} = 32000$ M^{-1} cm^{-1}) and 540 nm ($\varepsilon_{540} = 9000$ M^{-1} cm^{-1}) are recorded and the total heme concentration is computed. To insure that the species of interest is observed (oxy-, deoxy- or met-hemoglobin) the sample must be pretreated. In the case of reduced hemoglobin (oxy or deoxy) the standard is passed through a band of $Na_2S_2O_4$ in a Sephadex G-25 column [33]. The advantage of this method is that met-hemoglobin constantly encounters fresh reducing agent and that side reactions are limited by continued elution which quickly removes excess reagent from ferrous–hemoglobin. The determinations of met-hemoglobin extinction coefficients were conducted by subjecting the hemeprotein to autoxidation by atmospheric oxygen, by keeping the sample at 37°C for 24 h at pH 7.4.

Table 1 displays the determined extinction coefficients between 450 and 650 nm for the oxy-, deoxy- and met- fallow-deer hemoglobin species. A computer program based on these values was constructed to calculate the concentrations of oxygenated, deoxygenated and met-hemoglobin components in the mixed sample solution. Precise concentrations were determined to three significant figures after the addition of enzyme reducing system just before the beginning of the experiment. Hemoglobin concentrations were approximately 4 mM heme with around 1% met-hemoglobin present when the enzyme system was sufficiently active. To insure that the samples were free of net oxidation during the course of the experiment they were removed and analysed upon completion. This analysis revealed no more than 2% met formation at all temperatures.

Phosphate content was monitored spectrophotometrically through the formation of a phospho–molibdic complex [34]. In this procedure 50 μl of the purified hemoglobin sample are combined with 50 μl of a 10% $Mg(NO_3)_2 \cdot 6H_2O$ ethanol solution. The mixture is placed in a test tube and evaporated to dryness over a strong flame until brown fumes are no longer present. After cooling 300 μl of 1 M HCl are added, the tube is covered and placed in a water bath (95°C) for 15 min. This procedure converts any pyrophosphate that may have been formed into inorganic phosphate. The resulting inorganic phosphate is then analysed by adding 700 μl of an aqueous ascorbic acid–ammonium molybdate (1:6) mixture. This solution is kept at 45°C for 20 min and then the absorbance is taken at 820 nm using the extinction of $\varepsilon_{820} = 24000$ M^{-1} cm^{-1}.

2.2. Calorimetry

The calorimeter has been described previously [25] (see Fig. 1). Briefly, the main body of the calorimeter consists of an aluminum block which is shielded by an aluminum case enclosed in a chloro polyvinylchloride (CPVC) canister. Two thin walled flat bottom NMR tubes serve to connect the sample and reference cells to the dilution valve located at the top. A combination of thermopiles and resistance wires are used to measure reaction enthalpies using computer-controlled thermo-electrical compensation. The dilution valve is used to titrate gaseous ligands by way of successive logarithmic dilutions. The valve is equipped with an oxygen electrode which monitors the activity of oxygen while checking the system for leaks. Temperature is controlled by a Tronac regulated water bath with deviations less than ± 0.0003°C. The sample and reference solutions, measured by Hamilton syringe (typically 50.0 μl), are suspended on a piece of filter paper or glass membrane that is placed on the inside wall of a flat-bottom modified nuclear magnetic resonance (NMR) tube. These cells are inserted into the calorimeter and positioned within the copper cups.

The dilution valve operates by lowering the partial pressure of a reacting gas at constant temperature and pressure according to the following equation:

$$P_i = P_0 D^i \quad (2)$$

P_i is the partial pressure of a gas at dilution step i, P_0 is the starting pressure of the gas, and D is the dilution factor of the valve. Experiments are initiated, in the case of oxygen binding to hemoglobin, by first flushing the entire system with buffer-equi-

librated oxygen. After the system is flushed the bore of the valve is then turned toward the reaction and reference cells and the gas within the bore and cells is equilibrated to atmospheric pressure. The bore is then turned so that it is disconnected from the cells and an inert gas such as nitrogen is allowed to fill the bore until the oxygen electrode indicates completion. The valve is then turned into the cell, the nitrogen is equilibrated to atmospheric pressure and the partial pressure of oxygen is diluted according to Eq. 1. Logarithmic reductions in oxygen partial pressures are made by repeating the above sequence until the reaction is complete. The dilution factor can be determined by fitting the partial pressure of oxygen indicated by the oxygen electrode versus the nitrogen dilution step number. Gas dissolution heat effects are cancelled out by the placement of the enzyme system buffer in the reference cell.

2.3. Data analysis

The experiments conducted in this paper are ideally suited for analysis utilizing equilibrium and enthalpy expressions defined in the Adair formalism [35]. Thin-layer calorimetric heat binding data are taken in the form of enthalpy changes for a given change in partial pressure of oxygen. To fit this type of data the Adair representation is utilized to generate expressions that describe the enthalpy distribution as ligation occurs. We begin by depicting the four-site oxygen binding hemoglobin system by the series of equilibria:

$$Hb + O_2 \rightleftarrows HbO_2 \quad \Delta H_1, \beta_1 \tag{3}$$

$$Hb + 2O_2 \rightleftarrows Hb(O_2)_2 \quad \Delta H_2, \beta_2 \tag{4}$$

$$Hb + 3O_2 \rightleftarrows Hb(O_2)_3 \quad \Delta H_3, \beta_3 \tag{5}$$

$$Hb + 4O_2 \rightleftarrows Hb(O_2)_4 \quad \Delta H_4, \beta_4 \tag{6}$$

The ΔH's and β's are the overall enthalpies and equilibrium constants, respectively, for the given expressions. The average enthalpy of a macromolecule and the degree of ligand saturation can be treated in a parallel manner in a general statistical mechanical framework [36]. The hemoglobin oxygen binding macromolecular system is described in terms of the populations of its various ligated free energy levels [8]. The binding partition function or binding polynomial P, which is the sum of these states, can be expressed, taking the unligated macromolecule as the reference state, in terms of the above equilibrium constants β's and the ligand activity x [37].

$$P = 1 + \beta_1 x + \beta_2 x^2 + \beta_3 x^3 + \beta_4 x^4 \tag{7}$$

This binding polynomial in the Adair formalism is a function of the ligand activity and temperature. The temperature dependence of the overall binding constants β_j are given in terms of the overall enthalpies ΔH_j and the gas constant R:

$$\frac{\partial \ln \beta_j}{\partial (1/T)} = -\frac{\Delta H_j}{R} \tag{8}$$

The partition function or binding polynomial formalism can be utilized to generate expressions for the fractional saturation θ and the average enthalpy H (relative to the reference state H_0) by taking the appropriate derivatives of P:

$$\theta = \frac{1}{4}\left(\frac{\partial \ln P}{\partial \ln x}\right)_T \tag{9a}$$

$$\theta = \frac{\beta_1 x + 2\beta_2 x^2 + 3\beta_3 x^3 + 4\beta_4 x^4}{\left(1 + \beta_1 x + \beta_2 x^2 + \beta_3 x^3 + \beta_4 x^4\right)4} \tag{9b}$$

$$\overline{H} - \overline{H}_0 = -R\left(\frac{\partial \ln P}{\partial (1/T)}\right)_x \tag{10a}$$

$$\overline{H} - \overline{H}_0 = \frac{\Delta \overline{H}_1 \beta_1 x + \Delta \overline{H}_2 \beta_2 x^2 + \Delta \overline{H}_3 \beta_3 x^3 + \Delta \overline{H}_4 \beta_4 x^4}{1 + \beta_1 x + \beta_2 x^2 + \beta_3 x^3 + \beta_4 x^4} \tag{10b}$$

Eq. 9b, describing the fractional saturation, has been used in a number of optical studies [38–40] and Eq. 10b is the analogous enthalpy expression. As mentioned, experiments conducted with the gas-solution microcalorimeter described above yield differential heat binding curves in which the enthalpy change for a given oxygen partial pressure change is monitored. The theoretical reaction enthalpies for this type of experiment are given by

$$q_i^{\text{Theor}} = \left[\left(\overline{H} - \overline{H}_0\right)_i - \left(\overline{H} - \overline{H}_0\right)_{i-1}\right] C_{\text{Hb}} V \tag{11}$$

where q_i^{Theor} is the calculated heat at step i, C_{Hb} is the molar concentration of hemoglobin and V is the volume of the solution in liters.

When fitting the data, binding parameters are estimated by least-squares optimization using the Marquardt algorithm in which the experimentally measured enthalpies are compared with the theoretically calculated values and the standard deviation of the fit computed.

$$\sigma^2 = \frac{\sum_k \sum_i \left(q_i^{\text{exp}} - q_i^{\text{Theor}}\right)^2}{\nu} \qquad (12)$$

The additional summation k is added to allow for multiple data sets and ν is the number of degrees of freedom. The standard error of a point (SEP) gives a measure of the adequacy of the fit and is defined as the square root of the standard deviation. Parameter errors at the 67% confidence level are determined by use of the linear approximation of the curvature matrix [41]. The "true errors" (67% confidence level) are estimated by generating a series of 600 complete calorimetric binding curve data sets using parameter values corresponding to those determined by experiment. Each generated data set is given pseudo-random errors (consistent with the SEP) following a Gaussian distribution indicative of the experimental residuals. These simulations are individually fit and the average parameter errors are computed. This method of error analysis gives an indication of what the "true errors" would be if one could conduct the experiment a large number of times.

Initially, an attempt was made to fit individual single binding curve isotherms, but the eight free energy and enthalpy parameters proved to be too highly correlated to separate. As indicated, the temperature dependence of the equilibrium constants was exploited by conducting experiments at a number of different temperatures thereby expanding the data field. Simulations were performed to determine the number of binding curves necessary for parameter resolution at the approximate error level found in the experiment. These simulations indicated that three sets of three heat binding curves at 5°C intervals would be more than sufficient to over-determine the parameter values.

3. Results

In this study hemoglobin and buffer reducing system components are carefully controlled in order to minimize the heat effects exhibited by the various side reactions present in the reducing system cascade [24]. To verify the absence of these heat effects, experiments were performed with and without the system at 15°C where the oxidation of heme is minimal. The resulting heat binding curves were identical within the experimental error of the instrument. Higher temperature heat binding curves require the use of reducing system enzymes as met formation is evident over the course of the experiment. To monitor the influence of the reducing system at higher temperatures the overall enthalpies of oxygen binding were determined with and without enzyme at 20 and 25°C. This type of experiment can be conducted in a short period of time and the results indicated no significant difference in the total enthalpy. Another indication of the benign effect of the reducing system is the observation that the overall enthalpies were equal to the summation of the dilution enthalpies.

The solution conditions shown in Table 2 are chosen to minimize the effects associated with a number of possible side reactions in addition to those found with the enzyme reducing system. It is known that most hemoglobins display a large protonation effect upon oxygen binding (Bohr effect). By using phosphate to buffer the system the heat of protonation of buffer can be diminished. It is also characteristic of hemoglobins to dissociate into dimers at concentrations less than approximately 50 mM heme [42]. The high concentrations of hemoglobin chosen

Table 2
Experimental conditions

Buffer	Reducing system
4.05 mM heme 0.1 M potassium phosphate pH 7.4	2.0 mM glucose-6-phosphate 10 μM catalase 10 μM ferredoxin 100 μM NADPH 100 μM glucose-6-phosphate dehydrogenase 1.0 μM ferredoxin–$NADP^+$ reductase

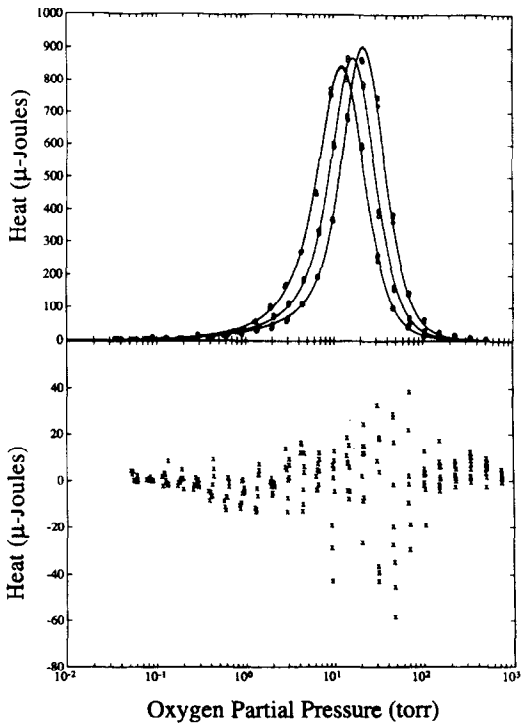

Fig. 2. Three heat binding experiments performed for fallow-deer hemoglobin at 15, 20 and 25°C, from left to right. Solid lines display the best fit function parameters at the appropriate temperatures and ligand activities. (A) Fallow-deer hemoglobin data and fitted function. (B) Residuals show the greatest errors in the middle of the binding curve due to longer compensation times and higher heats.

for our experiments effectively negate this effect while still allowing for rapid oxygen binding equilibration. Finally, as indicated previously, care is taken to remove all organic phosphates and other allosteric effectors such as chloride ions in order to simplify the system minimizing the number of extraneous heat effects.

Table 4
Calorimetric table of parameters for deer hemoglobin

Parameter	Value	Simulation errors
β_1	0.11 $Torr^{-1}$	± 0.039 $Torr^{-1}$
β_2	0.00056 $Torr^{-2}$	± 0.00048 $Torr^{-2}$
β_3	0.000061 $Torr^{-3}$	± 0.000015 $Torr^{-3}$
β_4	0.0000052 $Torr^{-4}$	± 0.0000023 $Torr^{-4}$
ΔH_1	−4.8 kcal/mol	± 1.3 kcal/mol
ΔH_2	−31.1 kcal/mol	± 4.8 kcal/mol
ΔH_3	−28.3 kcal/mol	± 3.0 kcal/mol
ΔH_4	−30.4 kcal/mol	± 0.16 kcal/mol
Maximum hill slope		2.37
P_m at 25°C		20.9 Torr

3.1. Calorimetric data

As mentioned above, in order to sufficiently define the data field, three heat binding curves were generated for fallow-deer hemoglobin at each of the chosen experimental temperatures (Fig. 2A). The temperatures 15, 20 and 25°C were used in order to maximize the stability of hemoglobin, allow for separation of binding curves and make possible rapid oxygen hemoglobin exchange. The fit of the data obtained by global computer analysis is shown in Fig. 2A and the SEP is found to be 12.5 μJ, which is reasonable for this type of instrument. The corresponding residuals are given in Fig. 2B. The residuals display the greatest error near the middle of the binding curve, and this effect is consistent with the longer thermal equilibration times and higher heats of reaction present in this region. The parameter

Table 3
Calorimetric cross-correlation matrix for the overall Adair constants and enthalpies for deer hemoglobin

	ΔH_1	ΔH_2	ΔH_3	ΔH_4	β_1	β_2	β_3	β_4
ΔH_1	1.000							
ΔH_2	0.9214	1.000						
ΔH_3	0.1726	−0.0688	1.000					
ΔH_4	0.1558	0.2074	−0.2578	1.000				
β_1	0.9650	0.8641	0.1369	0.0093	1.000			
β_2	0.9672	0.9719	0.1150	0.1496	0.9127	1.000		
β_3	0.1269	−0.0202	−0.1871	−0.2607	0.3016	−0.0577	1.000	
β_4	0.9778	0.8865	0.2021	0.0284	0.9789	0.9440	0.1905	1.000

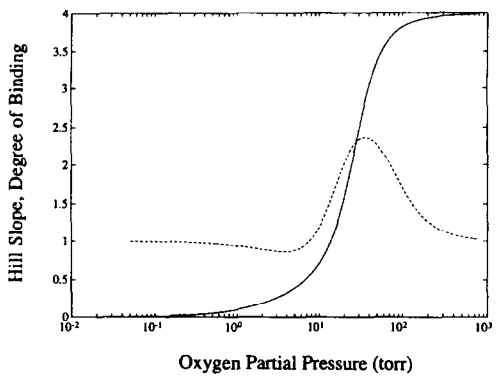

Fig. 3. The Hill slope at a given partial pressure of oxygen is given by the dashed line and the degree of binding by the solid line. The maximum Hill slope for fallow-deer hemoglobin is 2.37, the P_m is 20.9 Torr at 25°C.

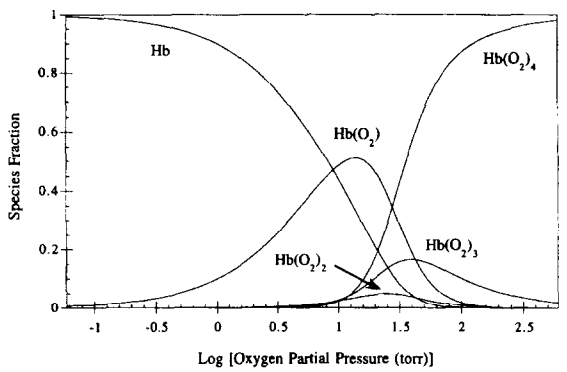

Fig. 4. Species fraction plot for fallow-deer hemoglobin reveals significant populations of all species with the doubly ligated having the smallest contribution.

cross-correlation matrix (Table 3) is related to the parameter dependence. The absolute value of the matrix off-diagonal components should be sufficiently below unity to warrant independence [43]. Even if the matrix does not represent a qualitative measure of correlation [44], it has been shown [45] that a fitting parameter can be solved from reasonably precise data if the pertinent cross-correlation coefficients are less than 0.98 (absolute value).

Errors were estimated by generating a series of 600 complete heat binding curve sets using parameter values corresponding to those of the experiments. To each generated data set pseudorandom errors were added following a Gaussian distribution. The resulting errors, obtained by fitting these simulations, are given in Table 4 along with the values of the parameters obtained from experiment. The maximum Hill slope is 2.37, the P_m at 25°C is 20.9 Torr and the Hill slope at the P_m is 2.07 (Fig. 3). The species fraction plots in Fig. 4 indicate the presence of significant populations of the four ligated species with the lowest fraction being the doubly ligated. This low doubly ligated characteristic was also obtained with studies conducted on bovine hemoglobin, while human hemoglobin displayed a low triply ligated species concentration. To highlight further the intermediate thermodynamics, the intrinsic stepwise parameters for fallow-deer hemoglobin are calculated from the overall values and are presented in Table 5.

4. Discussions

In our previous work [24] the overall enthalpies of oxygen and carbon monoxide binding to a number of species of myoglobins and hemoglobins were examined. As expected the overall binding of these ligands is shown to be exothermic and it is reasonable to assume that this enthalpy is the primary driving force of binding. However, examination of the intrinsic stepwise enthalpies of oxygen binding to various hemoglobins reveals the situation to be much more

Table 5
Intrinsic deer stepwise thermodynamics at 25°C

	$0 \rightarrow 1$ $Hb + O_2 \rightleftarrows HbO_2$	$1 \rightarrow 2$ $HbO_2 \rightleftarrows Hb(O_2)_2$	$2 \rightarrow 3$ $Hb(O_2)_2 + O_2 \rightleftarrows Hb(O_2)_3$	$3 \rightarrow 4$ $Hb(O_2)_3 + O_2 \rightleftarrows Hb(O_2)_4$
ΔH (kcal/mol)	-4.8 ± 1.3	-26.3 ± 5.0	2.8 ± 5.7	-2.1 ± 3.0
ΔG (kcal/mol)[a]	-5.8 ± 0.2	-4.5 ± 0.3	-6.8 ± 0.2	-7.3 ± 0.2
ΔS (cal/mol · K)	$+3.4 \pm 4.4$	-73.2 ± 16.8	$+32.2 \pm 19.1$	$+17.4 \pm 10.1$
$T\Delta S$ (kcal/mol)	$+1.0 \pm 1.3$	-21.8 ± 5.0	$+9.6 \pm 5.7$	$+5.2 \pm 3.0$

[a]All reactant and product concentrations are specified as molar in aqueous solution using 1.613 μM/Torr for the oxygen solubility at 25°C [49].

complicated. In fact, some of the ligation steps are found to have enthalpies much smaller in magnitude than what would be expected for myoglobin, which resembles the individual α and β subunits. In the extreme, bovine hemoglobin absorbs heat at the third ligation step indicating that the addition of a third oxygen is a highly entropy-driven process (Fig. 5). These types of radical deviations from the intrinsic myoglobin like enthalpy change are no doubt due to protonation effects and the variety of interactions occurring between and within the various subunits.

For fallow-deer hemoglobin the second stepwise oxygen binding step (Table 4) contains the majority of the enthalpy change (-26.3 ± 5.0 kcal/mol heme) with the first binding step having a smaller but appreciable enthalpy effect (-4.8 ± 1.3 kcal/mol heme). Of greater interest are the third and fourth intrinsic binding steps in that their enthalpy values are near zero ($+2.8 \pm 5.7$ and -2.1 ± 3.0 kcal/mol heme, respectively), indicating that the final two binding steps are entropy driven. These enthalpies, like those of other hemoglobins, have values that are much less exothermic than those determined for the non-cooperative binding of oxygen to myoglobin, -16.0 ± 0.05 kcal/mol heme. Although the deviation initially may seem excessive, the energetics associated with protein conformational changes [46], changes in salt bridges, and changes in the state of protonation [16] are more than sufficient to account for the effect.

In Figs. 5 and 6 the intrinsic stepwise thermodynamic parameters obtained for fallow-deer hemoglobin are compared with those determined for

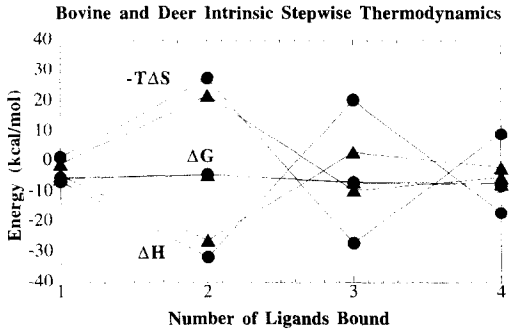

Fig. 5. Thermodynamic parameters for the intrinsic stepwise oxygenation of fallow-deer hemoglobin (triangles) compared with the values obtained for bovine hemoglobin (circles) [26].

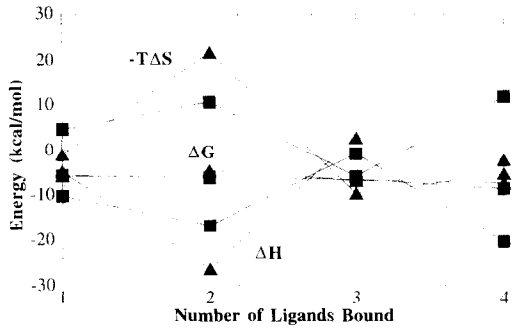

Fig. 6. Thermodynamic parameters for the intrinsic stepwise oxygenation of fallow-deer hemoglobin (triangles) compared with the values obtained for human hemoglobin (squares) [26].

human and bovine. It is interesting to note that the intrinsic stepwise free energies remain relatively constant as the enthalpy and entropy values exhibit large fluctuations. This type of enthalpy–entropy compensation is found in a number of physical processes including the energetics associated with protein unfolding. It has been speculated that the majority of the enthalpy difference between myoglobin and a number of the intrinsic hemoglobin oxygen binding steps is due to conformational changes resulting in the exposure or burial of amino acid surface area [47]. If this is the case then polar and apolar groups would have to be exposed in an asymmetric fashion as symmetric unfolding gives very low enthalpy values at room temperature (i.e. total protein unfolding shows little enthalpy change at 20°C). At present, structures of intermediate ligation states are yet unknown, so researchers have concentrated with limited success on the initial and final states of human hemoglobin as its oxy and deoxy structure have been determined. Fallow-deer hemoglobin's overall attenuation of the enthalpy change is larger than human's, so as structures become available, calculations involving the oxy and deoxy forms may prove to be more informative.

Another interesting aspect of these results is the apparent temperature insensitivity of oxygen affinity for the final two binding steps. Our analysis illustrates how temperature can be considered as a physical effector influencing gaseous ligand–hemoglobin complex stability. In the case of extreme environments, like the wide range of temperature changes that arctic mammals such as reindeer (*Rangifer*

tarandus) face in their living habitat, temperature is a physiologically relevant factor. Recent studies have outlined common features and different strategies for oxygen transport in critical environments [48], providing fascinating examples of macromolecular adaptation. Our interest in the study of fallow-deer hemoglobin is due to the fact that it does not live in an extreme environment, but is related to reindeer in the evolutionary sense. Fallow-deers (*Dama dama*) are ruminants belonging to the same family (*Cervidae*) as reindeer and thus one would expect that their oxygen transport molecules share a number of characteristics. We have shown that the intrinsic stepwise enthalpies are variable with the final two oxygen binding steps being relatively low in magnitude. This observation is in agreement with the results known for reindeer hemoglobin. It can be hypothesized that the high oxygen saturation states of these hemoglobins show insensitivity to temperature in order to allow consistent oxygen delivery at the level of peripheral tissues (skin, legs). This is important as the peripheral tissues of arctic mammals may be up to 10°C cooler than the lungs.

5. Conclusion

In this paper we have characterized the thermodynamics of oxygen binding to fallow-deer hemoglobin using the novel method of thin-layer gas-solution microcalorimetry. This technique does not rely on optical linearity of heme sites for the determination of binding constants and in addition offers direct enthalpy determination. We have shown that fallow-deer hemoglobin displays the same type of enthalpy–entropy compensatory binding effects found in human and bovine hemoglobins, while uniquely exhibiting minimal enthalpy changes for the final two oxygen binding steps. How this information relates to structural changes awaits the determination of intermediate ligation state structures most likely via NMR spectroscopy. As this intermediate structural information becomes available, the relationship between the structure and function of hemoglobins will become more specific resulting in models that may one day relate each energetic effect to a specific structural detail.

Acknowledgements

This work was supported by NIH grant RR-04328, GM-37911, NS-24520.

References

[1] D. Dolman and S.J. Gill, Anal. Biochem., 87 (1978) 127.
[2] B. Giardina, O. Brix, M. Nuutinen, S. Sherbini, A. Bardgard, G. Lazzarino and S. Condo, FEBS Lett., 247 (1989) 135.
[3] J.T. Edsall, Fed. Proc., 39 (1980) 226.
[4] J. Monod, Chance and Necessity, Chance, London, 1972.
[5] D.E. Koshland Jr., G. Nemethy and D. Filmer, Biochemistry, 5 (1966) 365.
[6] J. Monod, J. Wyman and J.P. Changeaux, J. Mol. Biol., 12 (1965) 88.
[7] J. Wyman, Adv. Protein Chem., 4 (1948) 407.
[8] J. Wyman, J. Am. Chem. Soc., 89 (1967) 2202.
[9] A. Colosimo, M. Brunori and J. Wyman, J. Mol. Biol., 100 (1976) 47.
[10] J. Wyman and S.J. Gill, Proc. Natl. Acad. Sci. USA, 77 (1980) 5239.
[11] E. Antonini and M. Brunori, Hemoglobin and Myoglobin in their Reactions with Ligands, North Holland, Amsterdam, 1971.
[12] M. Brunori, M. Coletta and B. Giardina, in P.M. Harrison (Ed.), Metalloproteins, Part 2: Metal Proteins with Non-redox Roles, MacMillan Press, London, 1985.
[13] J.M. Rifkind, Advances in Inorganic Biochemistry, Elsevier, New York, 1988.
[14] J. Baldwin and C. Chothia, J. Mol. Biol., 129 (1979) 175.
[15] R.E. Dickerson and I. Geis, Hemoglobin, Benjamin/Cummings, Menlo Park, CA, 1983.
[16] M.F. Perutz, Nature, 228 (1970) 726.
[17] M.F. Perutz, G. Fermi, B. Luisi, B. Shaanan and R.C. Liddington, Acc. Chem. Res., 20 (1987) 309.
[18] G.K. Ackers, M.L. Doyle, D. Meyers and M.A. Dougherty, Science, 255 (1992) 54.
[19] K. Imai, Allosteric Effects in Haemoglobin, Cambridge University Press, Cambridge, 1982.
[20] J. Wyman, Adv. Protein Chem., 19 (1964) 233.
[21] J. Wyman, Quart. Rev. Biophys., 17 (1984) 453.
[22] G.K. Ackers and J.H. Hazzard, TIBS, 18 (1993) 385.
[23] D.W. Ownby and S.J. Gill, Biophys. Chem., 37 (1990) 395.
[24] C.R. Johnson, S.J. Gill and K.S. Peters, Biophys. Chem., 45 (1992) 7.
[25] C.R. Johnson and S.J. Gill, Anal. Biochem., 209 (1993) 150.
[26] C.R. Johnson, D.W. Ownby, S.J. Gill and K.S. Peters, Biochemistry, 31 (1992) 10074.
[27] A. Riggs, Methods Enzymol., 76 (1981) 5.
[28] J.J. Christensen, L.D. Hansen and R.M. Izatt, Handbook of Proton Ionization Heats and Related Thermodynamic Quantities, Wiley, New York, 1976.

[29] A. Hayashi, T. Suzuki and M. Shin, Biochim. Biophys. Acta, 310 (1973) 309.
[30] R.E. Benesch, R. Benesch and S. Yung, Anal. Biochem., 55 (1973) 245.
[31] O.W. Van Assendelft and W.G. Zijlstra, Anal. Biochem., 69 (1975) 43.
[32] P.S. Chen, T.Y. Toribara and H. Warner, Anal. Chem., 28 (1956) 1756.
[33] B.F. Dixon and R. McIntosh, Nature, 28 (1967) 399.
[34] C. De Duve, Acta Chem. Scand., 2 (1948) 264.
[35] G.S. Adair, J. Biol. Chem., 63 (1925) 529.
[36] S.J. Gill, B. Richey, G. Bishop and J. Wyman, Biophys. Chem., 21 (1985) 1.
[37] J. Wyman and S.J. Gill, Binding and Linkage: The Functional Chemistry of Biological Macromolecules, University Science Books, Mill Valley, 1990.
[38] E. Bucci, C. Fronticelli and Z. Gryczynski, Biochemistry, 30 (1991) 3195.
[39] S.J. Gill, E. Di Cera, M.L. Doyle, G.A. Bishop and C.H. Robert, Biochemistry, 26 (1987) 3995.
[40] A. Parody-Morreale, C.H. Robert, G.A. Bishop and S.J. Gill, J. Biol. Chem., 262 (1987) 10994.
[41] P. Bevington, Data Reduction and Error Analysis for the Physical Sciences, McGraw-Hill, New York, 1969.
[42] F.C. Mills, M.L. Johnson and G.K. Ackers, Biochemistry, 15 (1976) 5350.
[43] M.E. Magar, Data Analysis in Biochemistry and Biophysics, Academic Press, New York, 1972.
[44] M.L. Johnson and S.G. Frasier, Methods Enzymol., 117 (1985) 301.
[45] M.L. Johnson, H.R. Halvorson and G.A. Ackers, Biochemistry, 15 (1976) 5363.
[46] C. Chothia, Nature, 248 (1974) 330.
[47] E. Bucci, C. Fronticelli, G. Zygmunt, A. Razynska and J.H. Collins, Biochemistry, 32 (1993) 3519.
[48] G. Di Prisco, S.G. Condo, M. Tamburrini and B. Giardina, TIBS, (1991) 471.
[49] D.M. Himmelblau, J. Chem. Eng. Data, 5 (1960) 10.